BIOPHARMACEUTICS & DRUG DISPOSITION
Biopharm. Drug Dispos. **33**: 179–194 (2012)
Published online 19 April 2012 in Wiley Online Library
(wileyonlinelibrary.com) **DOI**: 10.1002/bdd.1784

Predicting human hepatic clearance from *in vitro* drug metabolism and transport data: a scientific and pharmaceutical perspective for assessing drug–drug interactions

Gian Camenisch* and Ken-ichi Umehara
Drug–Drug Interaction Section, Drug Metabolism and Pharmacokinetics, Novartis Institutes of Biomedical Research, CH-4002, Basel, Switzerland

ABSTRACT: *Objectives:* Membrane transporters and metabolism are major determinants of the hepatobiliary elimination of drugs. This work investigates several key questions for drug development. Such questions include which drugs demonstrate transporter-based clearance in the clinic, and which *in vitro* methods are most suitable for drug classification, i.e. transporter- vs metabolism-dependent compound class categories. Additional questions posed are: what is the expected quantitative change in exposure in the presence of a transporter- and/or metabolism-inhibiting drug, and which criteria should trigger follow-up clinical drug–drug interaction studies. *Methods:* A well-established method for (human) liver clearance prediction that considers all four physiological processes driving hepatic drug elimination (namely sinusoidal uptake and efflux, metabolism and biliary secretion) was applied. Suspended hepatocytes, liver microsomes and sandwich-cultured hepatocytes were used as *in vitro* models to determine the individual intrinsic clearance for 13 selected compounds with various physicochemical and pharmacokinetic properties. *Results:* Using this *in vitro–in vivo* extrapolation method a good linear correlation was observed between predicted and reported human hepatic clearances. Linear regression analysis revealed much improved correlations compared with other prediction methods. *Conclusions:* The presented approach serves as a basis for accurate compound categorization within the Biopharmaceutics Drug Disposition Classification System (BDDCS) and was applied to anticipate metabolism- and transporter-based drug–drug interactions using different static prediction methods. A decision tree proposal is provided and helps to guide clinical studies on active processes influencing hepatic elimination. All recommendations in this paper are generally intended to support early pre-clinical and clinical drug development and the filing of a new drug application. Copyright © 2012 John Wiley & Sons, Ltd.

Key words: clearance prediction; drug–drug interactions; metabolism; transporter; compound classification

Introduction

Clearance (*CL*) is a parameter in pharmacokinetics (PK) that relates dose (*D*) to total drug exposure (*AUC*). The prediction of hepatic clearance in humans is particularly important as it provides an insight into the rate of elimination of a drug from the major clearance organ (liver). Many methods have been proposed for the prediction of human hepatic clearance from data in nonclinical species (allometry) or scale-up of *in vitro* data from human liver preparations. Most of the *in vitro* methods are based on single pathway analysis, focusing on either metabolism or sinusoidal hepatic uptake as the rate-limiting processes driving hepatic elimination [1,2]. Unfortunately, these single pathway

*Correspondence to: Drug–Drug Interaction Section (DDI), Drug Metabolism and Pharmacokinetics (DMPK), Novartis Institutes of Biomedical Research (NIBR), WSJ-153.2.02.01, CH-4002, Basel, Switzerland.
E-mail: gian.camenisch@novartis.com

Received 20 December 2011
Revised 24 February 2012
Accepted 6 March 2012

analysis methods often provide a poor correlation between predicted and observed clearances and rarely demonstrate a 1 to 1 change. Methods combining metabolism and transport data in a single system (e.g. sandwich-cultured hepatocytes) were also used, but the results do not always provide satisfying clearance predictions [3]. Improved *in vitro–in vivo* extrapolation (IVIVE) methods describe drug elimination from the liver cell as the interplay of uptake, metabolism, biliary secretion, and sinusoidal efflux [4–7]. Such a mechanism-based hepatobiliary elimination method was applied successfully to predict hepatic clearance in rats [3]. As shown by Sugiyama *et al*., the relative contribution of all the above pathways to the overall hepatic clearance of a drug is based primarily on whether transport(er)- or metabolism-mediated processes are the major factors fostering compound elimination [2,4]. As a result, the presence of process inhibitors may ultimately result in a quantitative change of the elimination rate (so called drug–drug interactions). A related conjecture by Benet and coworkers recognized that highly permeable compounds in general are also highly metabolized, whereas lowly permeable compounds are primarily actively excreted unchanged via the biliary and/or renal routes [8]. Based on these findings, a Biopharmaceutics Drug Disposition Classification System (BDDCS) has been devised to allocate drugs into four classes categorizing different routes of elimination.

The objective of this work was to illustrate the potential of this IVIVE method to accurately predict human hepatic clearances, to demonstrate the interrelationship between the mechanism-based hepatobiliary elimination model and the BDDCS classification, to evaluate its ability anticipating potential metabolism- and transporter-mediated drug–drug interactions (DDIs) in the clinic, and to highlight possible applicability in drug development.

Materials and Methods

In vitro clearance determination

The authors have recently published an IVIVE method to predict rat hepatic elimination based on *in vitro* clearances for uptake, metabolism, biliary secretion and sinusoidal efflux [3]. The same methods and calculation procedures were applied in the present study to generate corresponding human *in vitro* data for 13 compounds with various physicochemical and pharmacokinetic properties: propranolol, quinidine, verapamil, cyclosporine A, ketoconazole, atorvastatin, aliskiren, pravastatin, valsartan, cimetidine, digoxin, furosemide and ciprofloxacin. Briefly, hepatic uptake was determined in human hepatocytes at different concentrations (final concentrations: 1, 3, 10, 30 and 100 μM, except for cyclosporine A: 0.1, 0.3, 1, 3 and 10 μM) and incubation temperatures (37 °C or 4 °C) to determine uptake kinetics and non-specific binding. Cryopreserved pooled human hepatocytes (pool of ten donors, batch number HuP94) from Invitrogen Ltd (Paisley UK) were used throughout the study. The hepatocytes (viability: 77–89%) were suspended by using a hepatocyte one-step purification kit (BD Biosciences; San Jose, CA), and finally adjusted to 2.0×10^6 viable cells/ml with Krebs-Henseleit buffer (KHB). For the appraisal of hepatic metabolic clearance, a reaction mixture of the test compound at 6–8 concentrations (0.05–250 μM) in 100 mM phosphate buffer containing 5 mM $MgCl_2$ (pH 7.4) and NADPH (1 mM) was incubated with pooled human liver microsomes (pool of 50 donors, batch number 82087; BD Biosciences). Human sandwich-cultured hepatocytes (batch numbers: H-28APR10-02, H-22JUL10-01, H-28JUL10-01 and H-30JUL10-01) were used to assess the hepatobiliary disposition. The cells were purchased as a B-CLEAR®-RT kit from Qualyst, Inc. (Durham, NC) and were incubated at 37 °C with a compound solution in standard buffer at five different increasing concentrations (final concentrations: 1, 3, 10, 30 and 100 μM except for cyclosporine A: 0.1, 0.3, 1, 3 and 10 μM). From these experiments, the apparent biliary clearances as well as the sinusoidal efflux values (determined by a difference calculation) were derived as shown previously [3].

Mathematical theory and calculation methods

Considering all four processes driving hepatic drug elimination, based on the 'well-stirred liver' model, the hepatic clearance (CL_h) is described as follows [4,5,9]:

DOI: 10.1002/bdd

$$CL_h = \frac{Q_h \cdot f_{u,b} \cdot PS_{inf} \cdot \left(CL_{int,sec} + CL_{int,met}\right)}{Q_h \cdot \left(PS_{eff} + CL_{int,sec} + CL_{int,met}\right) + f_{u,b} \cdot PS_{inf} \cdot \left(CL_{int,sec} + CL_{int,met}\right)} \quad (1)$$

where Q_h represents the hepatic blood flow rate, $f_{u,b}$ is the fraction of drug unbound in the blood, $CL_{int,met}$ is the metabolic intrinsic clearance, PS_{inf} is the intrinsic membrane clearance for basolateral (sinusoidal) influx, PS_{eff} is the intrinsic clearance for efflux back into the blood at the sinusoidal membrane, and $CL_{int,sec}$ is the intrinsic membrane clearance for biliary secretion at the canalicular side of the hepatocytes.

Hence, the overall apparent (app) intrinsic clearance can be expressed as follows [4,10]:

$$CL_{int,app} = \frac{PS_{inf} \cdot \left(CL_{int,sec} + CL_{int,met}\right)}{PS_{eff} + \left(CL_{int,sec} + CL_{int,met}\right)} \quad (2)$$

Considering that transport processes at the sinusoidal membrane of hepatocytes may consist of a saturable (active, act) and a parallel non-saturable (passive, pas) component, Equation (2) can be rewritten (underlying assumption: the passive membrane clearance components for influx and efflux at the sinusoidal membrane are equal, i.e. $PS_{inf,pas} = PS_{eff,pas} = PS_{pas}$):

$$CL_{int,app} = \frac{\left(PS_{inf,act} + PS_{pas}\right) \cdot \left(CL_{int,sec} + CL_{int,met}\right)}{\left(PS_{eff,act} + PS_{pas}\right) + \left(CL_{int,sec} + CL_{int,met}\right)} \quad (3)$$

where $PS_{inf,act}$ and $PS_{eff,act}$ represent the active membrane clearances for hepatic influx and sinusoidal efflux, respectively.

Consequently, if the fraction of clearance which is affected by inhibition is designated f_m, and the unaffected fraction is $(1 - f_m)$, the following generalized equation describes the overall intrinsic hepatic clearance in the presence of potential process inhibitors (underlying premise: $CL_{int,sec}$ and $CL_{int,met}$ are solely active processes):

$$CL_{int,app,i} = \frac{\left(\left(1 - f_{m,inf}\right) \cdot PS_{inf,act} + PS_{pas}\right) \cdot \left(\left(1 - f_{m,sec}\right) \cdot CL_{int,sec} + \left(1 - f_{m,met}\right) \cdot CL_{int,met}\right)}{\left(\left(1 - f_{m,eff}\right) \cdot PS_{eff,act} + PS_{pas}\right) + \left(\left(1 - f_{m,sec}\right) \cdot CL_{int,sec} + \left(1 - f_{m,met}\right) \cdot CL_{int,met}\right)} \quad (4)$$

where $f_{m,x}$ is the fraction of active pathway x inhibited by the inhibitor.

Hypothetically, this model could be extended even further by taking into account that each of these active pathways can potentially be composed of several parallel processes all autonomously contributing to the apparent intrinsic clearance (e.g. $CL_{int,met} = CL_{int,met,enzyme1} + CL_{int,met,enzyme2}$).

Assuming that: (i) the substrate drug (victim) is not metabolized and/or transported in the intestine, (ii) Q_h, $f_{u,b}$ and the fraction of drug absorbed (F_a) do not change in the presence of an inhibitor (perpetrator), (iii) the liver is the only clearance organ and (iv) the inhibitor concentration does not vary with time, the ratio for the area under the exposure–time curve following oral application of a dose D in the presence ($AUC_{po,i}$) and absence (AUC_{po}) of the inhibitor drug can be defined as stated in Equation (5) [11,12]:

$$AUC_{po,i}/AUC_{po} = \frac{F_a \cdot F_{h,i} \cdot D/CL_{h,i}}{F_a \cdot F_h \cdot D/CL_h} = \frac{F_{h,i}/CL_{h,i}}{F_h/CL_h} = \frac{CL_{int,app}}{CL_{int,app,i}} \quad (5)$$

where F_h (= $1 - CL_h/Q_h$) and $F_{h,i}$ (= $1 - CL_{h,i}/Q_h$) are the fractions of an oral dose escaping hepatic first-pass in the absence and presence of inhibitor, respectively.

Data analysis

All (*in vitro*) data presented are averages of triplicate measurements. Predicted hepatic clearance and exposure change values were compared with observed values to determine the predictability of the methods described in this paper using standard statistical techniques. Following linear regression analysis the prediction accuracy was assessed by the coefficient of determination (R^2) and the precision was expressed by the intercept.

DOI: 10.1002/bdd

To identify the performance of the method, fold-error deviations between the predicted and observed values were calculated (% fold error < 2, < 3 and < 4).

Results

Human clearance prediction

Recent advances using *in vitro* technology allow quantitative measurements for each of the hepatic elimination processes described in Equation (3) [3]. Table 1 summarizes the *in vitro intrinsic* clearances for uptake, metabolism, biliary secretion and sinusoidal efflux determined in human microsomes and hepatocytes for the 13 selected compounds that have different class assignments according to BDDCS (Table 2). The clearances have been described previously for these compounds (in rat) following scale-up to a kg body weight basis in order to correct for the differences between the various *in vitro* assay systems. The scaled-up intrinsic clearance values for each individual process allowed for the overall determination of $CL_{int,app}$ according to Equation (3). Finally, the intrinsic clearances were substituted into Equation (1) to predict the corresponding *in vivo* hepatic clearances. As illustrated in Figure 1, this method reveals an excellent correlation between *in vivo* human hepatic clearance data obtained from the literature ($CL_{h,obs}$) and the predicted clearance values ($CL_{h,pred}$). Linear regression analysis provided an R^2 value of 0.817. The intercept was 0.337 and the slope could be determined with 0.881, which is close to the line of unity. The $CL_{h,pred}/CL_{h,obs}$ ratio was between 0.3 (ketoconazole) and 1.7 (ciprofloxacin). The prediction accuracy in terms of percentage within twofold, threefold and fourfold error was 85%, 92% and 100%, respectively. As recently demonstrated, this by far exceeds the accuracy and performance of all known prediction methods of human clearance based on non-clinical *in vivo* clearance data (allometry) and based on *in vitro* data [13]. While our prediction was generally very high for BDDCS class 1, 3 and 4 compounds, some class 2 compounds in the dataset (ketoconazole and atorvastatin) were notably underestimated for hepatic clearance. An underprediction of biliary secretion and/or an overprediction of sinusoidal efflux are the most likely explanation for this observation (both compounds are well-known efflux pump substrates). However, such underestimations of hepatic clearance for class 2 compounds were not observed previously in rats [3]. Yet, the possible limitations of the *in vitro* experiments (such as the assessment of unspecific binding events, the incorporation of controls, the choice of incubation times and pH conditions, etc.) and of the IVIVE approach in general (such as the selection of scaling factors across species, the assessment of variability, etc.) remain to be investigated further. Nonetheless, the presented results underline the power of this method to predict the *in vivo* (human) clearance of new chemical entities (NCEs).

Discussion

Compound categorization within BDDCS

Depending on the relative contributions of the individual elimination processes, based on Equation (2), different cases can be derived defining the slowest steps in the overall apparent intrinsic clearance [2,4]. In Figure 2 the resulting rate-limiting steps are represented. With the assumption that $CL_{int,sec}$ is small or negligible compared with $CL_{int,met}$, it becomes apparent that for all compounds permeating the sinusoidal membrane solely by passive diffusion as well as for all high permeability compounds where $PS_{eff} \approx PS_{inf} \approx PS_{pas}$ the main rate-determining clearance process in the liver is metabolism. For all other compounds, the sinusoidal and/or canalicular transporter effects are becoming increasingly important, though. This fundamental principle was also described previously by Wu and Benet, although their drug classification system (BDDCS) was mainly derived based on experimental observations rather than mathematical judgement [8,14]. The BDDCS was derived to evaluate for which compounds transporters must be investigated in order to understand intestinal absorption, organ disposition and potential drug–drug interactions of a drug. According to BDDCS, class 1 and 2 drugs are compounds with high (passive) permeability properties allowing them to cross physiological membranes, such as the plasma membrane of enterocytes in the gut or of

DOI: 10.1002/bdd

Table 1. Human hepatic clearances from *in vitro* assays and corresponding *in vivo* reference data

Compound	Influx		Metabolism	Biliary secretion	Efflux	Overall		Reference data				
	PS_{pas}	PS_{inf}	$CL_{int,met}$	$CL_{int,sec}$	PS_{eff}	$CL_{int,app}$	$CL_{h,pred}$	$CL_{h,obs}$	$CL_{h,pred}/CL_{h,obs}$	$CL_{met,obs}$	$f_{u,b}$	Literature
Propranolol	276.3	577.0	110.8	6.8	193.5	218.2	11.2	12.8	0.9	12.8	0.111	[31]
Quinidine	109.3	338.7	28.4	5.1	93.3	89.3	11.1	8.7	1.3	8.7	0.266	[32]
Verapamil	258.2	258.2	127.7	8.1	8.7	242.7	12.5	13.7	0.9	13.7	0.130	[33]
Cyclosporine A	41.9	155.1	77.6	9.1	108.6	68.9	1.9	3.1	0.6	3.0	0.030	[34]
Ketoconazole	1568.5	1568.5	97.4	29.6	2576.2	73.7	1.1	3.9	0.3	3.9	0.016	[35]
Atorvastatin	57.7	198.1	64.6	11.8	359.3	34.7	2.6	5.9	0.4	5.5	0.084	[29]
Aliskiren	25.4	57.7	89.2	31.2	134.4	27.3	9.9	11.3	0.9	1.5	0.699	[29]
Pravastatin	36.0	93.9	0.9	2.2	16.1	15.1	8.6	10.4	0.8	5.9	0.973	[36]
Valsartan	18.5	34.5	4.1	21.5	111.0	6.5	0.6	0.6	1.0	0.2	0.091	[37]
Cimetidine	3.6	6.6	528.7	0.2	3.6	6.6	4.3	2.7	1.6	2.4	0.835	[38]
Digoxin	6.9	26.9	24.2	18.4	102.2	7.9	4.9	4.6	1.1	0.6	0.815	[39]
Furosemide	23.9	35.0	19.0	1.2	77.7	7.2	0.2	0.4	0.5	0.2	0.032	[40]
Ciprofloxacin	22.9	29.9	22.0	0.0	14.0	18.3	7.8	4.5	1.7	1.4	0.686	[19]

All *intrinsic in vitro* clearances were determined and up-scaled to a ml/min/kg body weight basis as described previously [3]. The following scaling factors derived from literature were applied: 99 [10^6 cells/g liver] for suspended hepatocytes, 53 [mg protein/g liver] for liver microsomes, 116 [mg protein/g liver] for sandwich-cultured hepatocytes and 25.7 [g liver/kg body weight] for liver weight [41,42]. The overall apparent *intrinsic* hepatic clearance $CL_{int,app}$ was predicted according to Equation (3). The corresponding hepatic clearance $CL_{h,pred}$ was predicted according to Equation (1) (Q_h is 20.7 ml/min/kg). The *in vivo* metabolic clearances data ($CL_{met,obs}$) were calculated from *in vivo* human mass balance studies (% of parent) as given in the literature using the measured *in vivo* hepatic clearances ($CL_{h,obs}$) as the 100% reference.

DOI: 10.1002/bdd

Table 2. Compound classifications

Compound	BDDCS assignment according to Wu and Benet [8]	Subclass assignment according to decision tree in Figure 4	Class assignment according to decision tree in Figure 4
Propranolol	Class 1	Subclass 1/2	Class 2
Quinidine	Class 1	Subclass 1/2	Class 2
Verapamil	Class 1	Subclass 1/2	Class 2
Cyclosporine A	Class 2	Subclass 3/4	Class 4
Ketoconazole	Class 2	Subclass 1/2	Class 2
Atorvastatin	Class 2	Subclass 3/4	Class 4
Aliskiren	Class 3	Subclass 3/4	Class 4
Pravastatin	Class 3	Subclass 3/4	Class 4
Valsartan	Class 3	Subclass 3/4	Class 4
Cimetidine	Class 3	Subclass 3/4	Class 3
Digoxin	Class 4	Subclass 3/4	Class 4
Furosemide	Class 4	Subclass 3/4	Class 4
Ciprofloxacin	Class 4	Subclass 3/4	Class 3

The same dataset was selected as used previously in rats (exception BDDCS class 3 compound benzylpenicillin which, due to a lack of enough *in vivo* reference data, was replaced with cimetidine) [3].

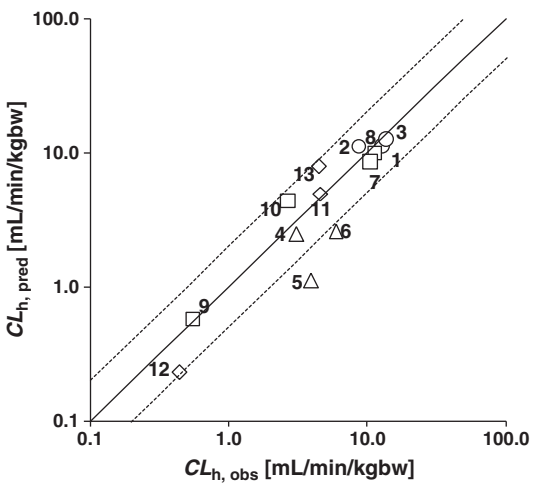

Figure 1. Comparison of the reported ($CL_{h,obs}$) and predicted ($CL_{h,pred}$) hepatic clearances in human as summarized in Table 1. Circles, triangles, squares and diamonds show the class 1, 2, 3 and 4 assignments according to BDDCS (Table 2), respectively. The solid line represents the line of unity and the dotted lines represent a two-fold error. The numbering of drugs is as follows: 1, propranolol; 2, quinidine; 3, verapamil; 4, cyclosporine A; 5, ketoconazole; 6, atorvastatin; 7, aliskiren; 8, pravastatin; 9, valsartan; 10, cimetidine; 11, digoxin; 12, furosemide; 13, ciprofloxacin

hepatocytes in the liver, easily. On the other hand, BDDCS class 3 and 4 compounds possess low permeability properties and therefore need specific uptake transporters not only for absorption in the gut, but also for uptake into hepatocytes. Due to low solubility, efflux effects can be important at the luminal side in the gut and at the sinusoidal membrane in the liver for class 2 and 4 compounds. Similarly, active biliary secretion of parent compound can be an important factor of disposition for class 3 and 4 compounds. Figure 2 illustrates the relationship between the mathematically derived mechanism-based hepatobiliary elimination model described above and the BDDCS as postulated by Wu and Benet. Both approaches recognize that the fundamental parameter controlling (hepatic) drug disposition is the compound-class dependent interplay between transporters, enzymes and membrane permeability. Figure 3 shows the estimated contribution of the measured *in vivo* metabolic clearance ($CL_{met,obs}$) to overall the *in vivo* hepatic clearance ($CL_{h,obs}$) for the 13 compounds in our dataset. As anticipated, the compounds in BDDCS classes 1 and 2 are predominantly cleared via metabolism, whereas the contribution of metabolic clearance to overall hepatic clearance generally decreases in classes 3 and 4.

Drugs with a high apparent hepatic intrinsic clearance are removed from the blood essentially as fast as they can be delivered to the liver, i.e. independent of protein binding and enzyme activities. Therefore, the elimination of such drugs is highly dependent upon liver blood flow and the inherent ability to cross the sinusoidal membrane rapidly. Consequently, according to the 'well-stirred liver' model, a compound can be ranked as highly permeable if $CL_{int,app} = PS_{pas} >> Q_h$ (Eqs 1 and 2). Thus, knowledge of the individual intrinsic clearances for active and passive uptake or sinusoidal efflux, metabolism and active biliary

DOI: 10.1002/bdd

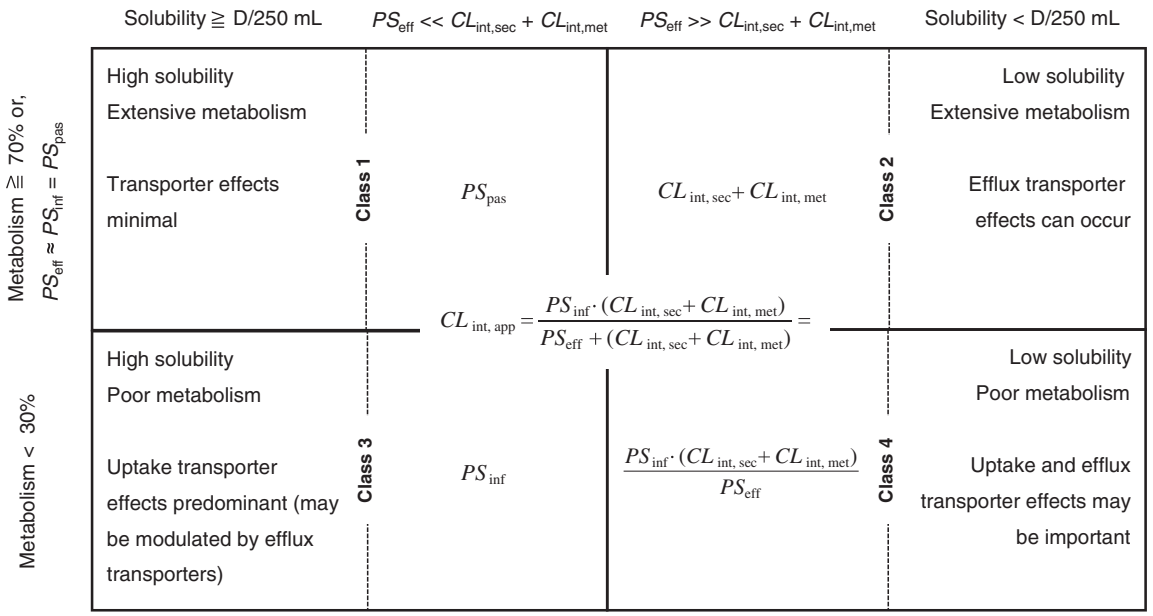

Figure 2. Summary of BDDCS and hepatobiliary liver model. The outer panels show the expected transporter effects on drug disposition for different drug classes as described by Wu and Benet [8]. The inner panels represent the equations for the apparent *intrinsic* hepatic clearance determination at different cases as indicated in the outlying area, taking into account the mechanism-based hepatobiliary elimination model according to Shitara *et al*. [4]

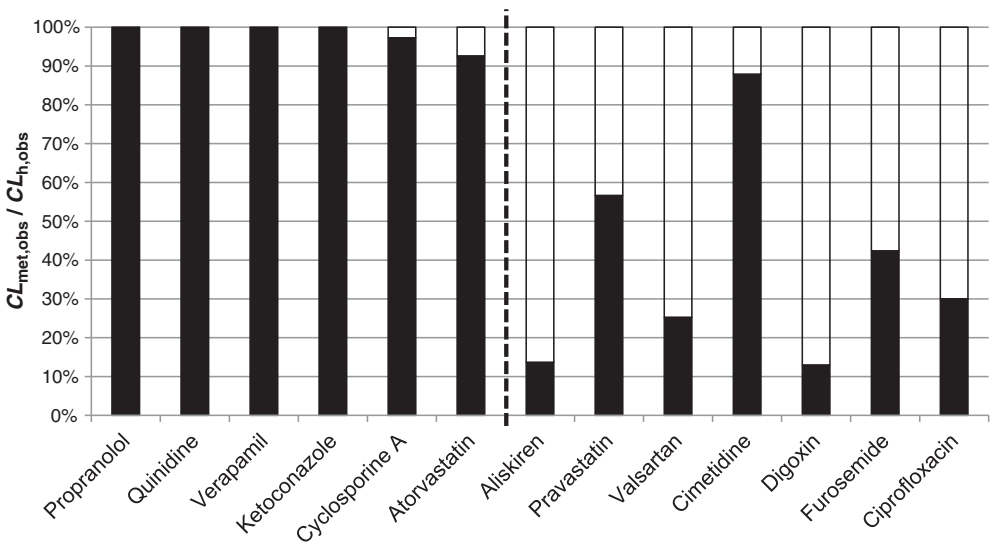

Figure 3. Contribution of *in vivo* metabolism (dark bars) to overall *in vivo* hepatic clearance according to Table 1. The dotted line separates the compounds with BDDCS class 1 and 2 assignment from those with BDDCS class 3 and 4 assignment according to Wu and Benet [8] (compare Table 2)

secretion will allow assignment to the four different BDDCS classes as shown in Figure 4. For a correct assignment of classes 1–4, all individual processes would still have to be assessed *in vitro*. However, only having knowledge of PS_{inf} and PS_{pas} already allows assignment to subclasses in

DOI: 10.1002/bdd

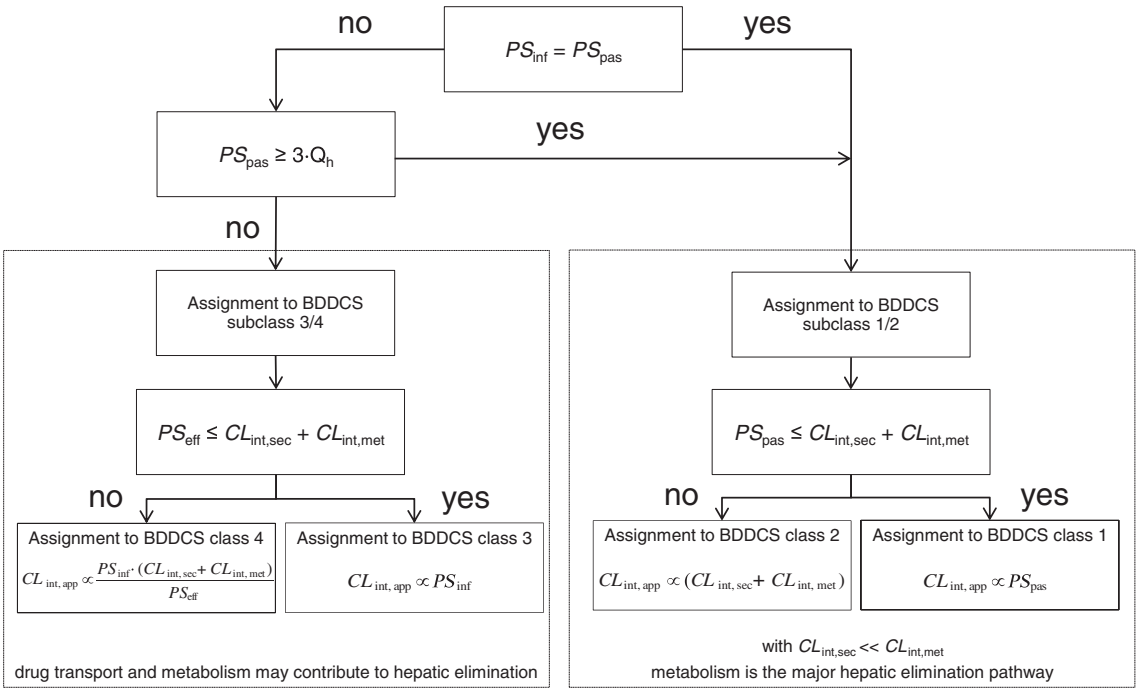

Figure 4. Decision tree for the assignment of new chemical entities to BDDCS compound (sub)classes based on scaled-up *in vitro* data (refer to Table 1). In the current assessment, compounds were assigned as highly permeable if PS_{pas} was ≥ 3-fold Q_h. The value for human hepatic clearance Q_h is 20.7 ml/min/kg

which metabolism (subclass 1/2) and combined transporter/metabolism activities (subclass 3/4) are the clearance determining processes, respectively. Both PS_{inf} and PS_{pas} can be derived from simple kinetic uptake experiments in suspended or plated primary hepatocytes as described previously [3]. Table 2 provides a summary of BDDCS assignment according to Wu and Benet and according to the decision tree outlined in Figure 4 for the heterogeneous dataset of 13 compounds listed in Table 1. With the exception of atorvastatin and cyclosporine A, a subclass assignment in line with the BDDCS could be performed for all compounds in the dataset. For approximately one-third of the compounds, class classification was the same as proposed by Wu and Benet (namely for ketoconazole, cimetidine, furosemide and digoxin). Except for ciprofloxacin, the remaining nine compounds using the proposed drug classification approach resulted in more stringent assignments than suggested by the BDDCS (e.g. the majority of BDDCS class 3 compounds were assigned to class 4). This apparent discrepancy between the two systems is not unexpected since: (i) the compound classification in Figure 4 vastly depends on the threshold that is set to define/identify the high permeability compounds (e.g. with $PS_{pas} \geq 2$-fold Q_h, thus all compounds in the dataset are assigned to the same subclasses as proposed by Wu and Benet) and, (ii) BDDCS assignments are based on the *in vivo* recognition of the elimination pathway as described in the literature (> 70% metabolism of an oral dose is considered as extensive metabolism), which can significantly deviate from the effective overall elimination mechanisms as shown above (e.g. atorvastatin is highly metabolized but the overall clearance is influenced to the same extent by active sinusoidal uptake and efflux transporters) and which, in human, is inherently difficult to quantify. Consequently, the above-mentioned limitations might lead to misclassification within either of the two classification systems. However, human *in vivo* data are not available during drug discovery. This generally limits or prohibits the applicability of the BDDCS system during earlier phases of drug development. Thus, an *in vitro* data based

DOI: 10.1002/bdd

classification method according to the decision tree in Figure 4 provides a valuable substitute, which is a key requirement for a compound class dependent clinical drug development programme (discussed in more detail below).

DDI predictions using the static $1-f_m$ approach

For compounds where the hepatic clearance is the major elimination route, using Equations (3), (4) and (5), the anticipated exposure change in the presence of perpetrator drugs can be expressed as:

$$AUC_{po,i}/AUC_{po} = \frac{PS_{inf}\cdot\left(CL_{int,sec}+CL_{int,met}\right)}{PS_{eff}+\left(CL_{int,sec}+CL_{int,met}\right)} \Big/ \frac{\left(\left(1-f_{m,inf}\right)\cdot PS_{inf,act}+PS_{pas}\right)\cdot\left(\left(1-f_{m,sec}\right)\cdot CL_{int,sec}+\left(1-f_{m,met}\right)\cdot CL_{int,met}\right)}{\left(\left(1-f_{m,eff}\right)\cdot PS_{eff,act}+PS_{pas}\right)+\left(\left(1-f_{m,sec}\right)\cdot CL_{int,sec}+\left(1-f_{m,met}\right)\cdot CL_{int,met}\right)} \quad (6)$$

with $PS_{eff} << (CL_{int,sec}+CL_{int,met})$ and $((1-f_{m,eff})\cdot PS_{eff,act}+PS_{pas}) << ((1-f_{m,sec})\cdot CL_{int,sec}+(1-f_{m,met})\cdot CL_{int,met})$ this relationship can be simplified as shown in Equation (7):

$$AUC_{po,i}/AUC_{po} = PS_{inf}/\left(\left(1-f_{m,inf}\right)\cdot PS_{inf,act}+PS_{pas}\right) \quad (7)$$

Similarly, with $PS_{eff} >> (CL_{int,sec}+CL_{int,met})$ and $((1-f_{m,eff})\cdot PS_{eff,act}+PS_{pas}) >> ((1-f_{m,sec})\cdot CL_{int,sec}+(1-f_{m,met})\cdot CL_{int,met})$ Equation (6) reduces to:

$$AUC_{po,i}/AUC_{po} = \frac{PS_{inf}\cdot\left(CL_{int,sec}+CL_{int,met}\right)}{PS_{eff}} \Big/ \frac{\left(\left(1-f_{m,inf}\right)\cdot PS_{inf,act}+PS_{pas}\right)\cdot\left(\left(1-f_{m,sec}\right)\cdot CL_{int,sec}+\left(1-f_{m,met}\right)\cdot CL_{int,met}\right)}{\left(\left(1-f_{m,eff}\right)\cdot PS_{eff,act}+PS_{pas}\right)} \quad (8)$$

As discussed above, for subclass 1/2 compounds active transport processes are likely to play a negligible role in drug elimination, and DDIs due to transporter inhibition are highly unlikely. Consequently, the anticipated exposure change of a subclass 1/2 compound can be estimated as a function of metabolism only as described by Equation (9):

$$AUC_{po,i}/AUC_{po} = CL_{int,met}/\left(\left(1-f_{m,met}\right)\cdot CL_{int,met}\right) = 1/\left(1-f_{m,met}\right) \quad (9)$$

This fundamental affiliation between major clearance pathways and potential implications for DDIs is summarized in Figure 5. Together, this new compound class assignment approach (see Figure 4) and the above relationships result in a straightforward assessment of the DDI potential of new drug candidates. Assuming *in vitro* processes are completely inhibited to their baseline (e.g. to PS_{pas} for hepatic uptake and sinusoidal efflux) based on Equations (6–9), maximal DDI estimates upon inhibition of each active elimination pathway x can be calculated to provide valuable information about the changes in fractional contributions in the presence of a perpetrator drug.

Table 3 provides a summary of the observed *in vivo AUC* changes in the presence of a selection of potential perpetrators for the class 4 compounds listed in Table 2 (exception digoxin) together with a series of different so-called static baseline predictions using Equation (6). From this analysis, the predicted *AUC* changes upon inhibition of several elimination pathways in parallel generally exceed the sum of the single pathways, emphasizing the complexity of the underlying process contributions (e.g. cyclosporine A – complete inhibition of hepatic active uptake is expected to change *AUC* about 3.7-fold and complete inhibition of metabolism is expected to change *AUC* about 3.3-fold, whereas maximal inhibition of both processes in parallel is predicted to increase *AUC* about 12.2-fold). Although possible but rather unlikely, parallel inhibition of all active processes promoting elimination ('worst-case' prediction) provides a ratio between predicted and observed *AUC* between 2.9 (pravastatin) and 14.1 (valsartan). Not surprisingly, considering only the fractional hepatic pathways of the victim drugs expected to interfere with the perpetrator compound, the predictions of exposure

DOI: 10.1002/bdd

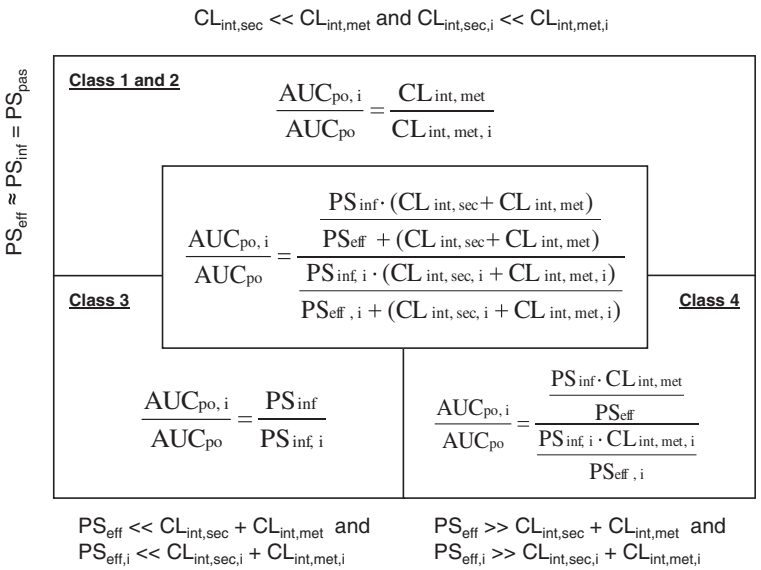

Figure 5. Compound class-dependent prediction of the DDI potential for drug substances taking into account the liver model for hepatobiliary elimination according to Shitara *et al*. [4]. Representation of Equations (6–9) for the compound class-dependent exposure change at different cases as indicated in the outlying area

change were much more accurate (between 0.9 (valsartan) and 3.8 (furosemide). The prediction accuracy in terms of percentage within twofold and fourfold error was 83% and 100%, respectively. With the help of fractional contributions for the different active processes (e.g. several enzymes that contribute together to overall metabolic clearance), this prediction accuracy could surely be improved even further. None of the static baseline predictions applied above provided a significant underestimation of the observed *in vivo* exposure changes. Based on Equation (5) such an underestimation of exposure changes could be expected for compounds with significant intestinal first-pass. Not surprisingly, a weak to mild contribution of intestinal metabolism to the overall oral bioavailability was demonstrated for all BDDCS class 2 and some class 4 compounds in our dataset [15–19]. Yet, the tendency to over-predict the observed *AUC* changes is evidentially directly associated with the nature of the estimation method (i.e. inhibition to the baseline) and also with the fact that possible alternative clearance pathways are neglected completely in this assessment (e.g. the contribution of renal clearance for valsartan, pravastatin and furosemide is reported to be about 30%, 45% and 80%, respectively). Nevertheless, especially the 'worst-case' prediction approach is offering a valuable option for early drug development allowing an appropriate risk evaluation, particularly for class 4 NCEs known to be eliminated in a rate-limited manner by the interplay of metabolic and transporter-mediated processes.

DDI predictions using the R-value approach

Physiologically based models use physiological and species-dependent parameters to describe concentration–time (PK) profiles [20]. As such, the integrated clearance prediction method discussed above represents a mechanistic physiologically based model of the liver [21,22]. The time dependency of the process should be also described within the physiologically based mathematical description. Furthermore, the interplay between the different processes involved in overall hepatobiliary transport must be linked to the appropriate varying substrate (S) and unbound inhibitor (I_u) concentrations within the relevant compartments (i.e. the hepatic input concentration in the portal vein (pv) as a function of time for the uptake process, and the corresponding intracellular concentration in the hepatocyte (hep) for the efflux, metabolism and biliary excretion process). As a result, physiologically based models have the capability of being more informative and

DOI: 10.1002/bdd

Table 3. Static baseline predictions for the assessment of DDI potential of class 4 compounds

Affected (victim) drug and processes known to be involved in its hepatic elimination	Inhibiting (perpetrator) drug and hepatic process known to be affected by them	Predicted *AUC* change assuming baseline inhibition of pathway(s) *x*							Measured *in vivo AUC* change	
		inf	met	sec	eff	all	worst-case	lit	obs	Literature
Cyclosporine A: CYP3A4, MDR1	Ketoconazole: CYPs, UGTs, OATPs, OCT1, MDR1, BSEP	3.7	**3.3**	**1.1**	0.7	9.6 (2.2)	22.2 (5.2)	6.0 (1.4)	4.3	[43]
Atorvastatin: CYP3A4, OATP1B1, NTCP, BCRP, MRP2, MDR1, MRP1	Rifampicin: OATPs, BSEP, MDR1, MRP2, MRP1	**3.4**	3.6	**1.1**	**0.3**	5.1 (2.0)	28.9 (11.6)	2.5 (1.0)	2.5	[44]
Aliskiren: CYP3A4, CYP2D6, OATP2B1, MDR1	Ketoconazole: CYPs, UGTs, OATPs, OCT1, MDR1	**2.3**	**2.1**	**1.2**	0.6	3.3 (1.8)	13.1 (7.3)	3.3 (1.8)	1.8	[45]
Pravastatin: CYP3A4, OATPs, OAT2, BCRP, MRP2	Cyclosporine A: CYPs, UGTs, NTCP, BCRP, MRP2, BSEP	2.6	**1.3**	**2.5**	2.0	49.3 (6.3)	22.3 (2.9)	8.5 (1.1)	7.8	[46]
Valsartan: CYP2C9, OATPs, MRP2, MDR1	Hydrochlorothiazide: -	1.9	1.1	3.5	0.3	2.9 (2.2)	15.5 (14.1)	1.0 (0.9)	1.1	[47]
Furosemide: UGTs, MRP2, BCRP	Probenecid: UGTs, OATPs, MDR1, MRP2, MRP1	1.5	**5.4**	**1.0**	0.5	3.9 (1.6)	11.9 (5.0)	8.1 (3.8)	2.4	[48]

Exposure changes are generally expressed as $AUC_{po,i}/AUC_{po}$ ratios according to Equation (6). The fractions of pathway *x* inhibited in the presence of an inhibitor were assumed to be as follows: $f_{m,inf} = f_{m,eff} = 1$ and $f_{m,met} = f_{m,sec} = 0.9$. The columns denominated with 'worst-case' and 'lit' provide the exposure change predictions considering a parallel inhibition of all active hepatic processes promoting elimination (all except sinusoidal efflux) and including only pathways known to be affected by the perpetrator drug and to interfere with the victim drug of interest as anticipated from the literature (bold numbers), respectively. In brackets the ratios between predicted and observed *AUC* changes are provided.

DOI: 10.1002/bdd

precise for interaction assessments compared with the static DDI prediction method described above. Assuming Michaelis-Menten kinetics, the concentration dependency for any active process can be described in the absence of an inhibitor drug as follows [23]:

$$PS_{\mathrm{x,act}} \text{ or } CL_{\mathrm{int,x,act}} = \frac{V_{\mathrm{max,x}}}{K_{\mathrm{m,x}} + S} \tag{10}$$

where $V_{\mathrm{max,x}}$ and $K_{\mathrm{m,x}}$ represent the maximum velocity and the affinity constant for the active pathway x, respectively.

In the presence of an inhibitor the active process clearances assuming a competitive inhibition mode can be described with:

$$PS_{\mathrm{x,act,i}} \text{ or } CL_{\mathrm{int,x,act,i}} = \frac{V_{\mathrm{max,x}}}{K_{\mathrm{m,x}} \cdot \left(1 + I_{\mathrm{u}}/K_{\mathrm{i,x}}\right) + S} \tag{11}$$

where $K_{\mathrm{i,x}}$ is the inhibition constant on pathway x for the perpetrator obtained from *in vitro* studies.

Consequently, the increase in exposure to the affected drug for an active process will be equal to [24]:

$$AUC_{\mathrm{po,i}}/AUC_{\mathrm{po}} = \frac{CL_{\mathrm{int,x,act}}}{CL_{\mathrm{int,x,act,i}}} = \frac{V_{\mathrm{max,x}}/\left(K_{\mathrm{m,x}} + S\right)}{V_{\mathrm{max,x}}/\left(K_{\mathrm{m,x}} \cdot \left(1 + \mathrm{I_u}/K_{\mathrm{i,x}}\right) + S\right)} \tag{12}$$

liver and kidney), and the non-eliminating tissue compartments (such as fat, muscle, etc.) and connects these by the circulatory system. Considering the potential complexity of this approach there are several commercial software tools available for the physiological modeling of pharmacokinetic processes including simulation of metabolism-based DDIs (e.g. Simcyp), which with the help of the above relationships could be expanded easily for transporter-mediated hepatobiliary elimination processes.

A major disadvantage of all physiologically based models is the need for a large number of *in vitro* and/or *in vivo* input parameters. Consequently, the preliminary assessment of the DDI potential of new molecular entities with less complex relationships is often applied as shown below:

For $S << K_{\mathrm{m,x}}$ Equations (10) and (11) can be simplified and Equation (12) reduces to:

$$AUCpo,i/AUCpo = 1 + \mathrm{I_u}/K_{\mathrm{i,x}} \tag{13}$$

From the above, it becomes evident that $1 - f_{\mathrm{m,x}}$ is equal to $1/(1 + I_{\mathrm{u}}/K_{\mathrm{i,x}})$. Consequently, Equation (4) can be rewritten as follows:

$$CL_{\mathrm{int,app,i}} = \frac{\left(PS_{\mathrm{inf,act}}/\left(1 + \mathrm{I_{u,pv}}/K_{\mathrm{i,inf}}\right) + PS_{\mathrm{pas}}\right) \cdot \left(CL_{\mathrm{int,sec}}/\left(1 + \mathrm{I_{u,hep}}/K_{\mathrm{i,sec}}\right) + CL_{\mathrm{int,met}}/\left(1 + \mathrm{I_{u,hep}}/K_{\mathrm{i,met}}\right)\right)}{\left(PS_{\mathrm{eff,act}}/\left(1 + \mathrm{I_{u,hep}}/K_{\mathrm{i,eff}}\right) + PS_{\mathrm{pas}}\right) + \left(CL_{\mathrm{int,sec}}/\left(1 + \mathrm{I_{u,hep}}/K_{\mathrm{i,sec}}\right) + CL_{\mathrm{int,met}}/\left(1 + \mathrm{I_{u,hep}}/K_{\mathrm{i,met}}\right)\right)} \tag{14}$$

This relationship becomes increasingly more complex when considering multiple active pathways as described by Equation (3). Since I_{u} and S are time-dependently reliant on the dosing regimen of victim and perpetrator drug as well as on other physiological variables influencing the concentration–time profiles, physiologically based liver models are often incorporated in more complex whole-body physiological models [20,25,26]. Whole-body models divide the body into anatomically and physiologically meaningful compartments, including the gastrointestinal tract for absorption, all eliminating organs (i.e. mainly

where $K_{\mathrm{i,inf}}$, $K_{\mathrm{i,eff}}$, $K_{\mathrm{i,sec}}$ and $K_{\mathrm{i,met}}$ are the (apparent) inhibition constants on the sinusoidal uptake, the sinusoidal efflux, the biliary secretion and the hepatic metabolism pathways, respectively. $I_{\mathrm{u,pv}}$ and $I_{\mathrm{u,hep}}$ are the unbound inhibitor concentrations within the portal vein and the hepatocytes, respectively.

The magnitude of interaction under this assumption is independent of S and lies only within the parameter I_{u}. However, both I_{u} and $K_{\mathrm{i,x}}$ are difficult to assess (even under static, time-independent conditions) especially in early drug discovery and become the limiting factors for the

DOI: 10.1002/bdd

in vivo prediction of DDIs [27]. Table 4 provides a static DDI prediction on the class 4 compound, atorvastatin, using the above integrated hepatobiliary $1 + I_u/K_{i,x}$ (*R*-value) approach for a series of perpetrator drugs for which the required IVIVE information could be located in the literature. The clinical drug–drug interaction potential was predicted to be most prominent for the perpetrator drug, amprenavir, followed by lopinavir, ritonavir and itraconazole, which is in line with the drug label information of these compounds [28,29]. The prediction accuracy for itraconazole was very high ($AUC_{po,i}/AUC_{po} = 1.7$) and provided a ratio between the predicted and observed *AUC* change of about 1.1 [30]. The predicted $AUC_{po,i}/AUC_{po}$ ratio of amprenavir (= 6.2) is about half of the corresponding baseline assessment (complete inhibition of metabolism and active sinusoidal uptake predicts an 12.5-fold *AUC* change). However, based on the $I_u/K_{i,x}$ ratio, the *R*-value method provides not only quantitative estimates but in addition projects the likelihood of an *in vivo* interaction and can therefore be considered as a valuable expansion of the static baseline approach discussed above. The individual *R*-values for amprenavir on CYP3A4, OATP1B1 and MDR1 were assessed with 30.6, 1.3 and 1.2, respectively. This supports the present hypothesis that the drug interaction potential of mainly class 4 compounds is often over- or underpredicted based on single pathway considerations.

Conclusion

In summary, the overall apparent intrinsic clearance estimates based on the hepatobiliary elimination model described in this paper can be used for the following: (i) *in vitro* data-based compound class assignment according to BDDCS, (ii) static prediction of the DDI potential of a NCE and (iii) elaboration of more complex pharmacokinetic (PK) models, e.g. deriving *in vivo* pharmacokinetic profiles, anticipating DDIs in a time-dependent manner or obtaining PK/PD relationships. Investigation of drug interactions on transporters can rarely be evaluated in isolation of the metabolism and *vice versa*. However, the relevance of transporters on elimination for highly permeable compounds becomes more and more negligible and

Table 4. Static DDI prediction on atorvastatin using the *R*-value ($1 + I_u/K_i$) approach

Victim drug	Perpetrator drug	PK parameter								K_i value			*AUC* change prediction	
		D (mg)	MW	$f_{u,p}$	k_a (min^{-1})	F_a	$I_{max,ss}$ (μM)	$I_{u,pv}$ (μM)	PS_{inf}/PS_{pas}	$I_{u,hep}$ (μM)	OATP1B1 (μM)	CYP3A4 (μM)	MDR1 (μM)	$AUC_{po,i}/AUC_{po}$	Literature
Atorvastatin	Lopinavir	400	629	0.015	0.03	1	15	0.23	2.2	0.50	0.1	0.41	~ 18	3.4	[28,49]
	Ritonavir	100	721	0.020	0.03	1	1.7	0.03	3.1	0.11	0.3	0.03	5	2.8	[28,49]
	Amprenavir	600	506	0.100	0.03	1	12	1.20	3.2	3.85	5.5	0.13	~ 20	6.2	[28,49]
	Itraconazole	200	706	0.010	0.62	1	0.9	0.01	1.0	0.01	-	0.01	0.2	1.7	[30,49]

All predictions of *AUC* changes were performed with Equation (5) using $CL_{int,app}$ and $CL_{int,app,i}$ estimates according to Equations (3) and (14), respectively. All estimates assume that the interaction potential is limited to hepatic processes only (hepatic clearance of atorvastatin is almost 100%) and that the fractions of the substrate transported by OATP1B1 or MDR1 and metabolized by CYP3A4 are 100%. The estimated maximum inhibitor concentration at the inlet of the liver (portal vein, pv) is estimated with [27]: $I_{u,pv} = f_{u,p} \cdot (I_{max,ss} + (F_a \cdot D \cdot k_a/Q_h))$, where F_a is the fraction of the inhibitor dose which is absorbed, k_a is the absorption rate constant of the inhibitor and $I_{max,ss}$ is the average *in vivo* steady-state plasma concentration of the inhibitor at dose *D*. The corresponding concentration within the hepatocytes can be assessed with: $I_{u,hep} = PS_{inf}/PS_{pas} \cdot I_{u,pv}$ where PS_{inf}/PS_{pas} is the hepatocyte accumulation factor determined *in vitro* as described previously [3].

DOI: 10.1002/bdd

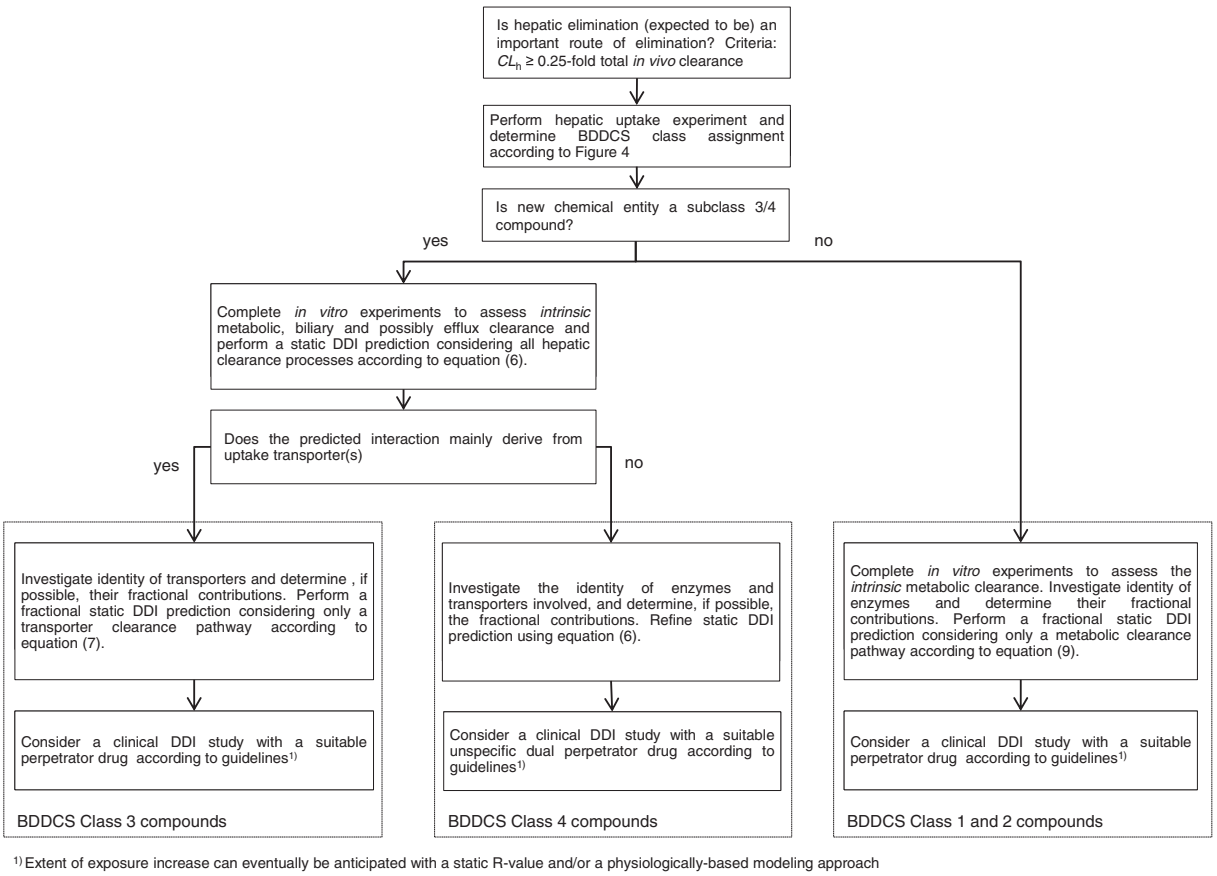

Figure 6. Proposal for a revised decision tree for hepatic elimination taking transporter and metabolism processes into account

metabolism becomes the rate-limiting process in overall hepatic clearance. Consequently, a correct compound class assignment in early development is the prerequisite for a compound-dependent, tailor-made pre-clinical and clinical follow-up programme in drug development. Figure 6 offers a proposal for a more integrated evaluation of the hepatobiliary interaction potential including potential follow-up activities. According to this decision tree, all subclass 1/2 compounds in the present dataset (propanolol, quinidine, verapamil, ketoconazole) require solely enzyme-based clinical interaction studies (compare Table 3). For the class 3 compounds, cimetidine and ciprofloxacin, DDI studies only on transporters are recommended. For all the remaining compounds, the static baseline prediction method suggests the quantitative involvement of transporters and metabolism (cyclosporine A, atorvastatin, aliskiren, pravastatin, valsartan, furosemide, digoxin). Thus, the use of nonspecific multiple inhibitors should be taken into consideration. However, limitations of this decision tree are currently not tested. Future research should include larger datasets, incorporate extrahepatic elimination pathways such as those for the kidney, integrate fractional contributions of parallel transporter and/or enzyme clearances and consider the involvement of intestinal processes.

Acknowledgements

The authors wish to acknowledge the many Novartis Drug Metabolism and Pharmacokinetic Department Scientists of Basel Switzerland who have supported the generation of data used in these analyses. Special thanks go to Drs Heike Gutmann, Joel Krauser and Birk Poller for their critical evaluation of this work.

DOI: 10.1002/bdd

Conflict of Interest

There is no potential conflict of interest for any author of this manuscript and there are no personal or financial relationships that might bias this work.

References

1. Ito K, Houston BJ. Comparison of the use of liver models for predicting drug clearance using *in vitro* kinetic data from hepatic microsomes and isolated hepatocytes. *Pharm Res* 2004; **21**: 785–792.
2. Watanabe T, Kusuhara H, Sugiyama Y. Application of physiologically based pharmacokinetic modeling and clearance concept to drugs showing transporter-mediated distribution and clearance in humans. *J Pharmacokinet Pharmacodyn* 2010; **37**: 575–590.
3. Umehara K, Camenisch G. Novel *in vitro–in vivo* extrapolation (IVIVE) method to predict hepatic organ clearance in rat. *Pharm Res* 2012; **29**: 603–617.
4. Shitara Y, Sato H, Sugiyama Y. Evaluation of drug–drug interaction in the hepatobiliary and renal transport of drugs. *Annu Rev Pharmacol Toxicol* 2005; **45**: 689–723.
5. Liu L, Pang S. The roles of transporters and enzymes in hepatic drug processing. *Drug Metab Dispos* 2005; **33**: 1–9.
6. Sirianni G, Pang S. Organ clearance concepts: New perspectives on old principles. *J Pharmcokinet Biopharm* 1997; **25**: 449–470.
7. Kwon Y, Morris ME. Membrane transport in hepatic clearance of drugs. I: Extended hepatic clearance models incorporating concentration-dependent transport and elimination processes. *Pharm Res* 1997; **14**: 774–779.
8. Wu CY, Benet LZ. Predicting drug disposition via application of BCS: transport/absorption/elimination interplay and development of a biopharmaceutics drug disposition classification system. *Pharm Res* 2005; **22**: 11–23.
9. Wilkinsin GR. Clearance approaches in pharmacology. *Pharmacol Rev* 1987; **39**: 1–47.
10. Yamazaki M, Suzuki H, Sugiyama Y. Recent advances in carrier-mediated hepatic uptake and biliary excretion of xenobiotics. *Pharm Res* 1996; **13**: 497–513.
11. Ito K, Iwatsubo T, Kanamitsu S, Ueda K, Suzuki H, Sugiyama Y. Prediction of pharmacokinetic alterations caused by drug–drug interactions: Metabolic interaction in the liver. *Pharmacol Rev* 1998; **50**: 387–411.
12. Einolf HJ. Comparison of different approaches to predict metabolic drug–drug interactions. *Xenobiotica* 2007; **37**: 1257–1294.
13. Ring B, Chien JY, Adkison KK, *et al*. PhRMA CPCDC initiative on predictive models of human pharmacokinetics, Part 3: Comparative assessment of prediction methods of human clearance. *J Pharm Sci* 2011; **100**: 4090–4110.
14. Custodio JM, Wu CY, Benet LZ. Predicting drug disposition, absorption/elimination /transporter interplay and the role of food on drug absorption. *Adv Drug Del Rev* 2008; **60**: 717–733.
15. Gertz M, Harrison A, Houston JB, Galetin A. Prediction of human intestinal first-pass metabolism of 25 CYP3A substrates from *in vitro* clearance and permeability data. *Drug Metab Dispos* 2010; **38**: 1147–1158.
16. Kadono K, Akabane T, Tabata K, Gato K, Terashita S, Teramura T. Quantitative prediction of intestinal metabolism in humans from a simplified intestinal availability model and empirical scaling factor. *Drug Metab Dispos* 2010; **38**: 1230–1237.
17. Huang YC, Colaizzi JL, Bierman RH, Woestenborghs R, Heykants J. Pharmacokinetics and dose proportionality of ketoconazole in normal volunteers. *Antimicrob Agents Chemother* 1986; **30**: 206–210.
18. Nishimuta H, Sato K, Yabuki M, Komuro S. Prediction of the intestinal first-pass metabolism of CYP3A and UGT substrates in humans from *in vitro* data. *Drug Metab Pharmacokinet* 2011; **26**: 592–601.
19. Vance-Bryan K, Guay DR, Rotschafer JC. Clinical pharmacokinetics of ciprofloxacin. *Clin Pharmacokinet* 1990; **19**: 434–461.
20. Lavé T, Parrott N, Grimm HP, Fleury A, Reddy M. Challenges and opportunities with modeling and simulation in drug discovery and drug development. *Xenobiotica* 2007; **37**: 1295–1310.
21. Poirier A, Funk C, Lavé T, Noé J. New strategies to address drug–drug interactions involving OATPs. *Curr Opinion Drug Dis and Dev* 2007; **10**: 74–83.
22. Kusuhara H, Sugiyama Y. *In vitro–in vivo* extrapolation of transporter-mediated clearance in the liver and kidney. *Drug Metab Pharmacokin* 2009; **24**: 37–52.
23. Rowland M, Martin SB. Kinetics of drug–drug interactions. *J Pharmacokinet Biopharm* 1973; **1**: 553–567.
24. Venkatakrishnan K, von Moltke LL, Obach RS, Greenblatt DJ. Drug metabolism and drug interactions: Application and clinical value of *in vitro* models. *Curr Drug Metab* 2036; **4**: 423–459.
25. Clewell HJ, Reddy MJ, Lavé T, Andersen ME. Physiologically based pharmacokinetic modeling. In *Preclinical Development Handbook*. Grad S (ed). John Wiley & Sons: Hoboken, NJ, 2007.
26. Rowland M, Balant L, Peck C. Physiologically based pharmacokinetics in drug development and regulatory science: A workshop report (Georgetown University, Washington DC, May 29–30, 2002). *AAPS Pharm Sci* 2004; **61**: E6.
27. Bachmann KA. Inhibition constants, inhibitor concentrations and the prediction of inhibitory drug

drug interactions: pitfalls, progress and promise. *Curr Drug Metab* 2006; **7**: 1–14.
28. International Transporter Consortium. Membrane transporters in drug development. *Nature Rev Drug Discov* 2010; **9**: 215–236.
29. Drugs@FDA database. www.accessdata.fda.gov/scripts/cder/drugsatfda/
30. Mazzu AL, Lassetter KC, Shamblen EC, Agarwal V, Lettieri J, Sundaressen P. Itraconazole alters the pharmacokinetics of atorvastatin to a greater extent than either cerivastatin or pravastatin. *Clin Pharmacol Ther* 2000; **68**: 391–400.
31. Walle T, Walle UK, Olanoff LS, Conradi EC. Partial metabolic clearances as determinants of the oral bioavailability of propranolol. *Br J Clin Pharmacol* 1986; **22**: 317–323.
32. Ochs HR, Greenblatt DJ, Woo E. Clinical pharmacokinetics of quinidine. *Clin Pharmacokinet* 1980; **5**: 150–168.
33. Eichelbaum M, Ende M, Remberg G, Schomerus M, Dengler HJ. The metabolism of DL-[14C] verapamil in man. *Drug Metab Dispos* 1979; **7**: 145–148.
34. Lemaire M, Maurer G, Wood AJ. Cyclosporin. Pharmacokinetics and metabolism. *Prog Allergy* 1986; **38**: 93–107.
35. Como JA, Dismukes WE. Oral azole drugs as systemic antifungal therapy. *N Engl J Med* 1995; **330**: 263–272.
36. Everett DW, Chando TJ, Didonato GC, Singhvi SM, Pan HY, Weinstein SH. Biotransformation of pravastatin sodium in humans. *Drug Metab Dispos* 1991; **19**: 740–748.
37. Waldmeier F, Flesch G, Müller P, *et al*. Pharmacokinetics, disposition and biotransformation of [14C]-radiolabelled valsartan in healthy male volunteers after a single oral dose. *Xenobiotica* 1997; **27**: 59–71.
38. Mitchell SC, Idle JR, Smith RL. The metabolism of [14C]cimetidine in man. *Xenobiotica* 1982; **12**: 283–292.
39. Doherty JE, Kane JJ. Clinical pharmacology of digitalis glycosides. *Annu Rev Med* 1975; **26**: 159–171.
40. Beermann B, Dalén E, Lindström B, Rosén A. On the fate of furosemide in man. *Eur J Clin Pharmacol* 1975; **9**: 51–61.
41. Carlile DJ, Zomorodi K, Houston JB. Scaling factors to relate drug metabolic clearance in hepatic microsomes, isolated hepatocytes, and the intact liver: studies with induced livers involving diazepam. *Drug Metab Dispos* 1997; **25**: 903–911.
42. Swift B, Pfeifer ND, Brouwer KL. Sandwich-cultured hepatocytes: an *in vitro* model to evaluate hepatobiliary transporter-based drug interactions and hepatotoxicity. *Drug Metab Rev* 2010; **42**: 446–471.
43. Foradori A, Mezzano S, Videla S, Pefaur J, Elberg A. Modification of the pharmacokinetics of cyclosporine A and metabolites by concomitant use of Neoral and diltiazem or ketoconazole in stable adult kidney transplants. *Transplant Proc* 1998; **30**: 1685–1687.
44. He YJ, Zhang W, Chen Y, *et al*. Rifampicin alters atorvastatin plasma concentrations on the basis of SLCO1B1 521 T > C polymorphism. *Clin Chim Acta* 2009; **405**: 49–52.
45. Vaidyanathan S, Camenisch G, Schuetz H, *et al*. Pharmacokinetics of the oral direct renin inhibitor aliskiren in combination with digoxin, atorvastatin, and ketoconazole in healthy subjects: the role of P-glycoprotein in the disposition of aliskiren. *J Clin Pharmacol* 2008; **48**: 1323–1338.
46. Park JW, Sieklmeier R, Merz M, *et al*. Pharmacokinetics of pravastatin in heart-transplant patients taking cyclosporine A. *Int J Clin Pharmacol Ther* 2002; **40**: 439–450.
47. Bhad P, Ayalasomayajula S, Kara R, *et al*. Evaluation of pharmacokinetic interactions between amlodipine, valsartan, and hydrochlorothiazide in patients with hypertension. *J Clin Pharmacol* 2011; **51**: 933–942.
48. Vree TB, van den Biggelaar-Martea M, Verwey-van Wissen CP. Probenecid inhibits the renal clearance of furosemide and its acyl glucuronide. *Br J Clin Pharmacol* 1995; **39**: 692–695.
49. University of Washington database. www.druginteractioninfo.org/

DOI: 10.1002/bdd